

Engineering Notes

ENGINEERING NOTES are short manuscripts describing new developments or important results of a preliminary nature. These Notes cannot exceed 6 manuscript pages and 3 figures; a page of text may be substituted for a figure and vice versa. After informal review by the editors, they may be published within a few months of the date of receipt. Style requirements are the same as for regular contributions (see inside back cover).

AIAA 82-4300

Calculated and Experimental Stress Distributions in a Ribbon Parachute Canopy

W.L. Garrard* and K.K. Muramoto†

University of Minnesota, Minneapolis, Minnesota

Introduction

IT is important to be able to accurately predict loads and stresses in parachute structures. If parachute structural loads are underestimated in the design stage, system failures may result during flight testing and expensive design modifications and retesting may be required. On the other hand, if structural loads are overestimated or if unnecessarily large factors of safety are applied to compensate for uncertainties in the accuracy of load and stress calculations, parachute systems of excessive weight and volume will result.

During the Apollo program, Mullins et al.¹ and Reynolds et al.² developed a finite-element procedure and a computer code named CANO for analysis of the loads and stresses in slotted parachutes. The CANO program has since been used in the successful design of a number of high performance parachute systems³; however, despite the successful use of CANO, there has been no experimental verification of the stresses calculated using the program. In fact to the authors' knowledge there has been no comparison of measured and calculated canopy stresses for any type of parachute canopy or for any theory for the prediction of canopy stresses. This is due to the fact that until recently no experimental measurements of stresses in parachute canopies had been successfully performed. In 1981, Konicke and Garrard⁴ succeeded in measuring canopy stresses in a wind tunnel model of a ribbon parachute using Omega stress sensors. In this Note, the steady-state canopy stress distributions calculated using a modified version of the CANO program⁵ are compared with the distribution as measured by Konicke and Garrard. The measured and calculated stress distributions are reasonably close except for a region about two-thirds the distance from the vent to the skirt. Also, the distribution of maximum circumferential loads calculated using CANO for a high performance lifting ribbon parachute³ was normalized and compared with the distribution of maximum normalized stress measured by Konicke and Garrard. Although there are a number of differences in the two parachutes, the distributions are very close except near the skirt.

Calculated and Experimental Stress Distribution

Experimental canopy stress measurements were performed by Konicke and Garrard⁴ on a 4.50-ft-diam flat ribbon

parachute of 20% geometric porosity constructed from 1.1 oz/yd² nylon of 4% effective porosity. Omega sensors were mounted along the centerline of one of the gores to measure circumferential stress and an electronic force balance was used to measure overall axial force on the parachute. The parachute was disreefed and inflated in the wind tunnel under infinite mass conditions. Canopy stresses and drag were measured as functions of time until steady state was reached. The details of the experimental procedure are described in Ref. 4. The measured steady-state stress distribution for a dynamic pressure of 4.16 psf is shown in Fig. 1.

Circumferential stresses were calculated for this condition using CANO. The basic inputs required by CANO were 1) the parachute geometry and material characteristics, 2) the measured axial force acting on the parachute, and 3) the differential canopy pressure coefficients at a maximum of nine radial positions from the vent to the skirt. Since Konicke and Garrard were unable to make differential pressure measurements on their canopy, differential pressure coefficients reported by Melzig and Schmidt,⁶ Pepper and Reed,⁷ and Heinrich and Uotila⁸ were used. These pressure distributions are shown in Fig. 2. The tests by Melzig and Schmidt closely approximated those of Konicke and Garrard in the sense that both model parachutes were similar and both tests were run at relatively low dynamic pressures (from 4.16 to 7.28 psf for Konicke and Garrard and from 5.83 to 30.45 psf for Melzig and Schmidt). Both parachutes were flat and were constructed of 24 gores with 27 ribbons per gore. The parachute used by Melzig and Schmidt had a diameter of 4.46 ft and porosity of 18%. Both parachutes were constructed of cloth of the same nominal porosity; however, the parachute of Melzig and Schmidt was constructed of 1.45 oz/yd² cloth and was therefore heavier and less flexible than the parachute used by Konicke and Garrard.

Pepper and Reed⁷ reported results for 24-gore, 20-deg conical ribbon parachutes with a range of geometric porosities. Testing was conducted over a range of dynamic pressures in two wind tunnels. The parachute diameters were 3 ft and the parachutes were of heavier construction than the one used by Konicke and Garrard. Differential pressure coefficients for a 25% geometric porosity parachute tested at a dynamic pressure of 75 psf were used as input to CANO since this pressure distribution approximated the shape of the measured canopy stress distribution.

Heinrich and Uotila⁸ presented a detailed analysis of additional data collected by Pepper and Reed but not given in Ref. 7. The pressure distribution for a 20% geometric porosity ribbon parachute tested at 50 psf was selected for use in CANO as this parachute and test condition was closest to the parachute and test condition reported by Konicke and Garrard.

The stresses calculated using the three pressure distributions as described above as input to CANO are compared with the measured distribution in Fig. 1. Experimental and calculated values compare well in the skirt and vent regions but diverge at about two-thirds the distance from the vent to the skirt. The calculated values are somewhat higher than the measured values in this region. There is considerable variation between the stress distributions calculated using the three pressure distributions. This is not surprising since the parachutes used by Pepper and Reed were of conical construction, whereas the one used by Konicke and Garrard was flat. The parachute and test conditions used by Melzig and Schmidt were similar to

Received Jan. 15, 1982; revision received June 11, 1982. Copyright © American Institute of Aeronautics and Astronautics, Inc., 1982. All rights reserved.

*Associate Professor, Department of Aerospace Engineering and Mechanics. Associate Fellow AIAA.

†Graduate Research Assistant, Department of Aerospace Engineering and Mechanics.

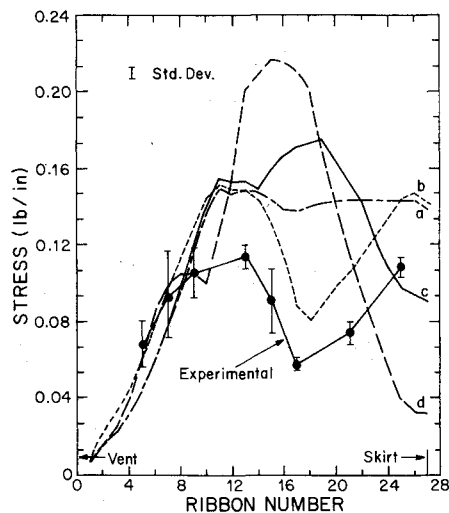


Fig. 1 Experimental and calculated steady-state canopy stress vs ribbon number. Calculated stress computed using differential pressure coefficients from a) Melzig and Schmidt, b) postulated, c) Heinrich and Uotila, d) Pepper and Reed.

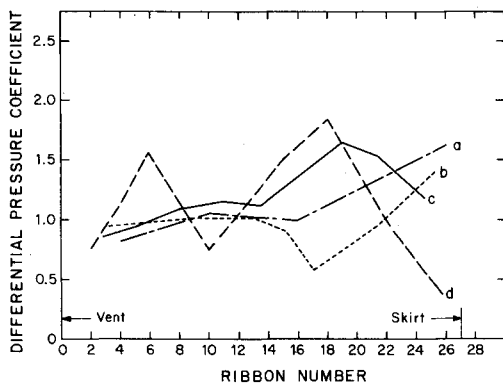


Fig. 2 Distribution of differential pressure coefficients used in calculation of steady-state canopy stress: a) Melzig and Schmidt, b) postulated, c) Heinrich and Uotila, d) Pepper and Reed.

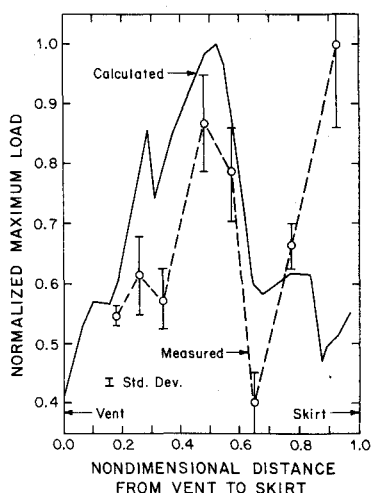


Fig. 3 Comparison of computed and measured distributions of normalized maximum ribbon load during inflation.

those of Konicke and Garrard and the results obtained from this pressure distribution were closest to the measured values. Unfortunately Melzig and Schmidt measured pressure at only four points on the parachute and no data were given in the region of greatest discrepancy between calculated and measured values of stress. CANO performs a linear interpolation on the pressure distribution between data points and lack of a data point in the region between ribbons 16 and

26 could account for much of the difference between the measured and calculated stress distributions. Also the parachute used by Konicke and Garrard was more flexible than those used in the pressure distribution studies and the inflated shape could have been somewhat different from the inflated shapes of the parachutes used in the pressure distribution studies. Relatively small changes in geometry often result in large changes in pressure distribution, and as can be seen from Figs. 1 and 2, the stress distribution is very sensitive to the pressure distribution.

In an attempt to calculate a stress distribution identical to the measured distribution, various distributions of pressure coefficients were used as an input to CANO. Twenty-five pressure distributions were examined and the best results obtained, the postulated distributions, are shown in Figs. 1 and 2. As can be seen, the calculated and experimental stress distributions are very close.

The postulated pressure distribution is very close to the pressure distribution given by Melzig and Schmidt except in the region near ribbons 16-22. In this region the postulated pressure coefficients are small resulting in small values of stress. In the vent region the ribbons are nearly perpendicular to the airflow, the aerodynamic forces are due to drag, and the resulting stresses are fairly high. In the skirt region the angle of attack of the ribbons is such that considerable lift is generated accounting for the high stresses in this region. In the area where low stresses are observed, ribbons 16-22, the angle of attack of the ribbons is large enough so that the ribbons are effectively stalled and little lift is generated. During testing it was observed that the inflated canopy was relatively "soft" in this region. It was necessary to relax the convergence criterion at the vent in order to obtain a converged solution with CANO using the postulated pressure distribution.

Meyer, Klimas, and Wolf³ used CANO to calculate the forces in the ribbons of a lifting ribbon parachute during inflation. Loads were calculated using several pressure distributions representing various stages of inflation and the maximum load calculated in each ribbon was tabulated. These results were normalized by dividing by the peak load and are compared in Fig. 3 with the normalized maximum loads reported by Konicke and Garrard. The distributions are very close except near the skirt.

Conclusions

The results reported in this paper provide the first quantitative comparison of ribbon parachute canopy stresses calculated using the CANO program and experimentally measured stresses. At steady state the calculated and measured values of maximum stress are encouragingly close. Measured and calculated distributions of maximum stress during inflation also compare very well except near the skirt. It is felt these variations are due to the fact that the pressure distributions used in the calculations were not taken under the same test conditions as those used for the stress measurements. Research in which pressure and stress distributions are simultaneously measured is currently underway.

Acknowledgment

This research was supported by Sandia National Laboratories under Contract 73-0540.

References

- ¹Mullins, W.M., Reynolds, D.T., Lindh, K.G., and Bottoroff, M.R., "Investigation of Prediction Methods for the Loads and Stresses of Apollo Type Spacecraft Parachutes Volume II—Stresses," Northrop Corp. NVR-6432, Newbury Park, Calif., June 1970.
- ²Reynolds, D.T. and Mullins, W.M., "Stress Analysis of Ribbon Parachutes," AIAA Paper 75-1372, Nov. 1975.
- ³Meyers, S.D., Klimas, P.C., and Wolf, D.F., "Structural Analysis and Design of a High Performance Lifting Ribbon Parachute," AIAA Paper 79-0428, March 1979.

⁴Konicke, T.A. and Garrard, W.L., "Stress Measurements in a Ribbon Parachute Canopy During Inflation and at Steady State," AIAA Paper 81-1944, Oct. 1981; see also *Journal of Aircraft*, Vol. 19, July 1982, pp. 598-600.

⁵Muramoto, K. K. and Garrard, W. L., "A Users Manual for CANO 2," Report No. SAND-81-03, Department of Aerospace Engineering and Mechanics, University of Minnesota, Minneapolis, Minn., Jan. 1982.

⁶Melzig, H.D. and Schmidt, P.K., "Pressure Distribution During Parachute Opening, Phase I. Infinite Mass Operating Case," AF-FDL-TR-66-10, March 1966.

⁷Pepper, W.B. and Reed, J.F., "Parametric Study of Parachute Pressure Distribution by Wind Tunnel Testing," *Journal of Aircraft*, Vol. 13, Nov. 1976, pp. 895-900.

⁸Heinrich, H.G. and Uotila, J., "Pressure and Profile Data of 20° Conical Ribbon Parachutes," Sandia National Laboratories Report SAND-17-7005, May 1977.

AIAA 82-4301

Wall Interference Evaluation from Pressure Measurements on Control Surfaces

R. Gopinath*

NASA Langley Research Center, Hampton, Virginia

Nomenclature

A	= constant in Eq. (8)
C_p	= pressure coefficient
f_H	= defined by Eq. (3)
f_B	= defined by Eq. (4)
h	= test section height
M_∞	= freestream Mach number
q	= source strength
x, y	= physical coordinates
α	= geometrical angle of attack
β	$= \sqrt{1 - M_\infty^2}$
γ	= vortex strength
ΔM	= Mach number correction
$\Delta \alpha$	= angle-of-attack correction
μ	= doublet strength
ξ	$= x$
ϕ_m	= far-field perturbation potential

Subscripts

B	= bottom wall
H	= top wall

Introduction

CONVENTIONAL methods of calculating wall interference corrections are based on boundary conditions which require a knowledge of the porosity parameter for ventilated walls and are not suitable for deformed walls. The correction methods are uncertain and, on occasion, inadequate. In some methods, the ventilated walls are regarded as imaginary walls with uniform characteristics which are estimated through numerical simulations or wind tunnel experiments. These methods have not been uniformly successful. This is particularly true where nonlinear effects are important, such as when the model is not small enough compared to the height of the tunnel, the incidence is large, or the flow is high subsonic.

A method proposed by Capelier, Chevallier, and Bouniol¹ dispenses with the need to resort to additional tests to determine the porosity characteristics and replaces them by pressure measurements on a control surface near each wall of a wind tunnel. The method is valid only for subcritical flows or for flows with weak shocks. Like the classical methods, it represents the model by singularities which are deduced from its geometry and measured forces. This method can be applied to all types of walls, permeable or solid, flat or deformed.

Mokry and Ohman² have used a method similar in principle to the approach of Ref. 1, but different in the selection of boundaries and implementation of the integration of wall pressures. It utilizes the Fourier solution of the Dirichlet problem for a finite rectangular region. It requires only the value of the flow angle at a selected reference point sufficiently distant from the airfoil.

In view of the scatter in wall pressure measurements, the data were smoothed using cubic splines before calculating the values of the boundary functions, but it was found that the method was relatively insensitive to the smoothing factor. As the evaluation of interference corrections by the method of Ref. 1 requires that the pressure distribution be known along the entire length of the control surface extending from upstream to downstream infinity, an attempt was made to evaluate the contributions from the regions beyond the extent of experimental pressure measurements to $\pm \infty$ by trying out various types of pressure distributions.

The present method uses a simple exponential decay of pressure distribution beyond the most upstream and downstream limits in order to evaluate the expressions for the Mach number and incidence corrections as given by Ref. 1. It is satisfying to note that the incidence correction checks surprisingly well with Mokry's³ results for a BGK-1 airfoil at $M_\infty = 0.784$ and 2.56 deg, even without the reference value of incidence. The upstream contribution to incidence correction is considerable and cannot be ignored. The upstream and downstream contributions to Mach number correction are negligible. Numerical experiments were made with various types of variations for C_p beyond the experimental range of pressure measurements and the exponential decay of pressure was found to be appropriate.

Method of Solution

The final expressions for Mach number and incidence correction¹ are

$$\Delta M = \left(\frac{1}{\beta h} \right) \int_{-\infty}^{+\infty} \frac{f_B(\xi) + f_H(\xi)}{2 \cosh(\pi \xi / \beta h)} d\xi \quad (1)$$

$$\Delta \alpha = \left(\frac{1}{h} \right) \int_{-\infty}^{+\infty} \frac{f_H(\xi) - f_B(\xi)}{1 + \exp(2\pi \xi / \beta h)} d\xi \quad (2)$$

where

$$f_H(\xi) = -\frac{1}{2} C_{pH}(\xi) - \left(\frac{\partial \phi_m}{\partial x} \right)_H \quad (3)$$

$$f_B(\xi) = -\frac{1}{2} C_{pB}(\xi) - \left(\frac{\partial \phi_m}{\partial x} \right)_B \quad (4)$$

For a thin lifting airfoil in subsonic linearized flow, ϕ_m is given by

$$\phi_m = - \left(\frac{\gamma}{2\pi} \right) \arctan \left(\frac{\beta y}{x} \right) + \left(\frac{\mu}{2\pi\beta} \right) \frac{x}{x^2 + \beta^2 y^2} + \frac{1}{2} \left(\frac{q}{2\pi\beta} \right) \ln(x^2 + \beta^2 y^2) \quad (5)$$

Differentiating Eq. (5) with respect to x , substituting in Eqs. (3) and (4), and simplifying, the final expressions for ΔM

Received May 29, 1982; revision received July 19, 1982. Copyright © American Institute of Aeronautics and Astronautics, Inc., 1982. All rights reserved.

*National Research Council Associate.